MABS
2018, VOL. 10, NO. 7, 992–1002
https://doi.org/10.1080/19420862.2018.1496879

Taylor & Francis
Taylor & Francis Group

REPORT

Platform development for expression and purification of stable isotope labeled monoclonal antibodies in *Escherichia coli*

Prasad T. Reddy[a], Robert G. Brinson[b], J. Todd Hoopes[a], Colleen McClung [c], Na Ke[c], Lila Kashi[a], Mehmet Berkmen [c], and Zvi Kelman[a]

[a]Biomolecular Labeling Laboratory, Institute for Bioscience and Biotechnology Research, National Institute of Standards and Technology and the University of Maryland, Rockville, MD, USA; [b]Institute for Bioscience and Biotechnology Research, National Institute of Standards and Technology and the University of Maryland, Rockville, MD, USA; [c]New England Biolabs, Ipswich, MA, USA

ABSTRACT

The widespread use of monoclonal antibodies (mAbs) as a platform for therapeutic drug development in the pharmaceutical industry has led to an increased interest in robust experimental approaches for assessment of mAb structure, stability and dynamics. The ability to enrich proteins with stable isotopes is a prerequisite for the in-depth application of many structural and biophysical methods, including nuclear magnetic resonance (NMR), small angle neutron scattering, neutron reflectometry, and quantitative mass spectrometry. While mAbs can typically be produced with very high yields using mammalian cell expression, stable isotope labeling using cell culture is expensive and often impractical. The most common and cost-efficient approach to label proteins is to express proteins in *Escherichia coli* grown in minimal media; however, such methods for mAbs have not been reported to date. Here we present, for the first time, the expression and purification of a stable isotope labeled mAb from a genetically engineered *E. coli* strain capable of forming disulfide bonds in its cytoplasm. It is shown using two-dimensional NMR spectral fingerprinting that the unlabeled mAb and the mAb singly or triply labeled with ^{13}C, ^{15}N, ^{2}H are well folded, with only minor structural differences relative to the mammalian cell-produced mAb that are attributed to the lack of glycosylation in the Fc domain. This advancement of an *E. coli*-based mAb expression platform will facilitate the production of mAbs for in-depth structural characterization, including the high resolution investigation of mechanisms of action.

ARTICLE HISTORY
Received 22 February 2018
Revised 26 June 2018
Accepted 27 June 2018

KEYWORDS
Deuterium labeling; monoclonal antibody; nuclear magnetic resonance (NMR); protein labeling; stable isotope labeling

Introduction

Monoclonal antibodies (mAbs) represent an important platform for development of biotherapeutic products.[1,2] These proteins are typically expressed in mammalian cell lines to enable glycosylation, which plays an important role in mAb function and stability.[3] In-depth characterization of mAb structure and dynamics using techniques such as nuclear magnetic resonance spectroscopy (NMR), small angle neutron scattering (SANS) neutron reflectometry (NR) and quantitative mass spectroscopy is highly desirable. However, enrichment of proteins with stable isotopes is a prerequisite for in-depth application of these structural and biophysical methods. To date, expression in mammalian cell lines, which is typical for mAbs, has not proven to be a practical and cost effective path to obtaining such stable isotope labeled samples. *Escherichia coli* is the most common platform for production of stable isotopically labeled proteins (e.g., ^{2}H, ^{13}C, and ^{15}N)[4,5] and nucleic acids[6] due to the ability of bacteria to grow in well-defined minimal media, including fully deuterated media. The minimal media contains only salts and an energy source (usually glucose or glycerol) and does not require supplementation with either amino acid or nucleic acids.

Several reports are available for the production of an intact mAb in rich media involving the co-expression of a chaperone protein.[7–14] However, to date, no protocols have been developed for expression and purification of full-length mAbs from *E. coli* grown in minimal media. The only protocol reported in the literature is for the expression and purification of the Fc.[15] The development of such a system would greatly enhance the study of the structure and dynamics of mAbs.

Here we describe, for the first time, the expression and purification of full-length labeled National Institute of Standards and Technology mAb (NISTmAb) in a genetically engineered *E. coli* strain called SHuffle.[16,17] The NISTmAb is an IgG1κ antibody that was expressed by its originator in mammalian cells. It is a well-characterized test material that has been made widely available to facilitate the development of both originator biologics and biosimilars.[2,18,19] The large amount of publically available data for the NISTmAb makes it an ideal choice for use as a model system for development of new stable isotopic labeling production platforms that are efficient and cost effective. For this study, the SHuffle strains have been engineered for the expression of the periplasmic disulfide bond isomerase DsbC in the cytoplasm, greatly enhancing the fidelity of correct disulfide bond formation.[16,17]

CONTACT Prasad T. Reddy prasad.reddy@nist.gov NIST/IBBR 9600 Gudelsky Drive, Rockville, MD 20850
Color versions of one or more of the figures in the article can be found online at www.tandfonline.com/kmab.
Supplemental data for this article can be accessed here.

These strains have their reductive pathways genetically deleted, permitting the formation of disulfide bonds in proteins that require it for their folding. Using a SHuffle strain, we show intact mAb production in *E. coli* by demonstrating that the NISTmAb (herein designated as eNISTmAb for the aglycosylated protein produced from *E. coli*) can be either singly or triply labeled with ^{2}H, ^{13}C, or ^{15}N.

Results

Cytoplasmic production of mAb

Use of native *E. coli* for heterologous expression of proteins in the cytoplasm is not conducive to disulfide bond formation due to the presence of disulfide bond reductases,[20] and therefore secretion of the protein to the periplasm, which harbors disulfide bond oxidase DsbA, is required. Expression of mAbs in native *E. coli* cells in rich media has previously been shown to result in the production of purified, well-folded, full-length mAb in the periplasm.[11,12] Following this precedent, our initial strategy to produce labeled mAb in native *E. coli* using minimal media involved the use of several constructs that encode the heavy and light chains downstream of a signal peptide for secretion into the periplasm. Initial attempts, however, to express the mAb in minimal media in the periplasm yielded no observed, purified product.

Our expression strategy was then changed to production of the protein in the cytoplasm. For proper formation of disulfide bonds, the SHuffle T7 cells were identified as a potential expression platform because the cells are engineered to overproduce a cytoplasmic version of disulfide bond isomerase (DsbC).[16] In addition to the expression of DsbC, the cells also express the T7 RNA polymerase, and therefore can be adapted to all expression vectors that depend upon either T7 or *E. coli* RNA polymerases. Using the SHuffle T7 platform and purification of eNISTmAb from crude extract by affinity chromatography with Protein-A or CaptureSelect CH1 domain resins (see Materials and Methods for details), the performance of the platform was evaluated using sodium dodecyl sulfate polyacrylamide gel electrophoresis (SDS-PAGE). As expected, the heavy chain and light chain of the full-length mAb are observed under reducing conditions of the SDS-PAGE analysis (Figure 1). The size of the *E. coli*-expressed heavy chain, however, is smaller than the NISTmAb expressed in eukaryotic cells (Figure 1 compare lanes 1–3 to lane 4). This observation is likely due to glycosylation of the heavy chain in eukaryotic cells, which does not occur in bacteria. To determine if glycosylation is responsible for the slower migration of the NISTmAb heavy chain, an aglycosylated form of the NISTmAb was generated using PNGase F as previously described.[21] As shown in Figure 2, the migration of the eNISTmAb heavy chain is similar to the aglycosylated form of the NISTmAb heavy chain (Figure 2, compare lane 3 to lane 2), suggesting that the faster migration of the eNISTmAb heavy chain is due to the lack of glycosylation. Subsequent mass spectral analysis confirmed that the intact masses of the heavy and light chains matched the theoretical

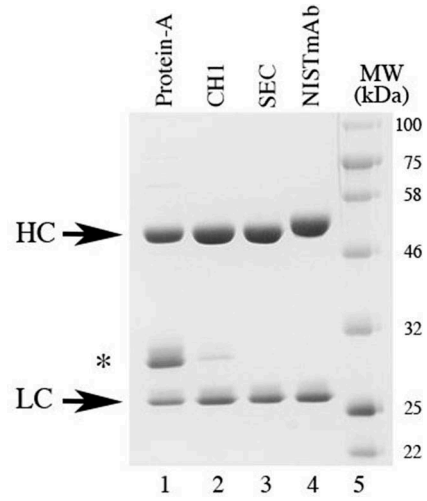

Figure 1. SDS-PAGE analysis of eNISTmAb purification steps.

SDS-PAGE analysis of the eNISTmAb after purification on Protein-A (lane 1) or CH1 (lane 2) column and after SEC purification of the eluted proteins from the Protein-A column (lane 3). NISTmAb was used as a reference (lane 4). Five micrograms of each protein were separated on a 10% SDS-PAGE followed by staining with Coomassie Brilliant Blue R-250. Lane 5, molecular weight marker (kDa); HC, heavy chain; LC, light chain, *, truncated heavy chain.

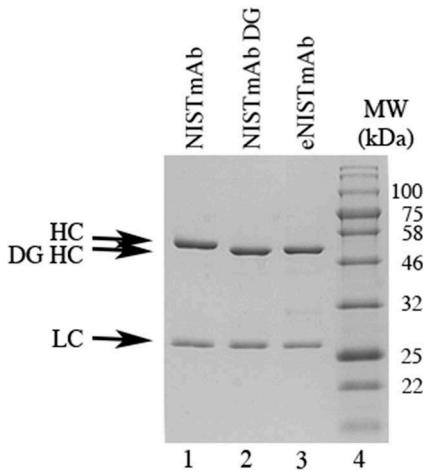

Figure 2. SDS-PAGE comparison of the NISTmAb, deglycosylated NISTmAb and the eNISTmAb.

Two and half microgram of the NISTmAb (lane 1), deglycosylated NISTmAb (lane 2) and eNISTmAb (lane 3) were separated on a 12% SDS-PAGE followed by staining with Coomassie Brilliant Blue R-250. Lane 4, molecular weight marker (kDa); HC, heavy chain; LC, light chain, DG HC, deglycosylated NISTmAb heavy chain.

masses. The observed molecular mass of the light chain was 23,257.0 Da, with a theoretical molecular mass of 23,259.0 Da, and the observed molecular mass of the heavy chain was 49,735.34 Da, with a theoretical molecular mass of 49,738.5 Da, indicating the correct synthesis of both chains (Figure 3A and B). The eNISTmAb was expressed in *E. coli* without a signal peptide. As translation starts with methionine, the intact mass includes Met at the N-termini of the light and heavy chains.

In addition to the full-length eNISTmAb (Fig. S1A and B), a putative truncated product of the heavy chain was also observed (marked by an asterisk in Figure 1, Fig. S2; see also Figure 3A). This product was much more pronounced when the mAb was

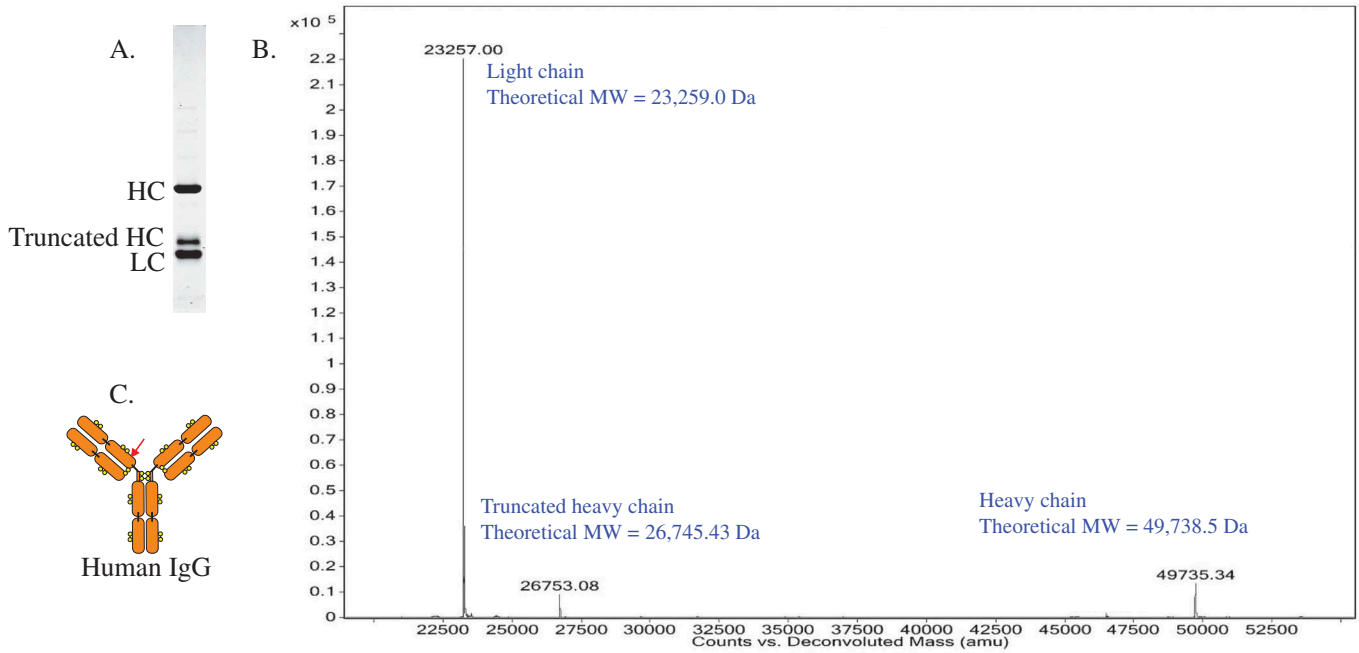

Figure 3. Mass-spec analysis of the purified eNISTmAb.

A) SDS-PAGE analysis of the purified eNISTmAb after purification on Protein-A column. HC, heavy chain; LC, light chain, Truncated HC, truncated heavy chain. B) The intact molecular weight of the heavy and light chains and the truncated heavy chain were determined by reverse phase LC-MS analysis as described in Materials and Methods. The expected theoretical molecular weights are shown in blue (see text for details). C) The location of the truncation on a schematic representation of mAb is shown by an arrow.

purified on Protein-A resin in comparison to CaptureSelect C_H1 resin (Figure 1, compare lane 1 to lane 2), suggesting that the truncation is on the Fab part of the molecule (Figure 3C). Mass spectral analysis of the truncated product suggested that the truncation occurred in the C_H1 region of the heavy chain (Fig. S2). To determine the identity of the putative truncated product, N-terminal Edman sequencing was conducted. The resulting sequence of MDKRVEPKS matched the native heavy chain sequence of VDKRVEPKS, with a valine to methionine substitution at the N-terminus of the truncated protein (Fig. S3). The theoretical molecular mass of truncated product starting with MDKRVEPKS (26,745.43 Da) matched the observed molecular mass (26,753.08 Da) (Figure 3B), strongly supporting the hypothesis that a Val_{214} to M substitution occurred. These observations lead to the hypothesis that the truncation of the heavy chain could be explained by an internal translation initiation at the valine codon (GTG), which has been measured *in vivo* to be approximately 10% of all start sites in *E. coli*.[22–24] Since less truncation product was co-purified with the full-length antibody on CaptureSelect C_H1 resin, this resin was used for several of the subsequent purifications of ^{15}N, ^{13}C, ^{2}H and the triply labeled eNISTmAbs.

Most protein translation in *E. coli* initiates by binding of the ribosome at the ribosome binding site (RBS) on the mRNA. The RBS, also referred to as the Shine-Dalgarno (SD) sequence, is located 5–10 bases upstream of the start codon. This is predominantly ATG and accounts for about 85% of initiation sites in bacteria. Other, less frequent, initiation sites are also used, including GTG and TTG. However, not all bacterial genes contain a RBS, and other mechanisms initiate translation of those genes.[25] Scanning the RNA sequence upstream of the putative internal GTG initiation site did not identify any clear SD sequence. To confirm that the truncation product observed (Figure 1, lane 1) is the result of internal translation initiation and not due to another reason, the GTG codon was replaced with GTT. While both GTG and GTT encode for Val, only GTG is known to function as an initiation codon. As shown in Figure 4, the protein purified on Protein-A column from cells expressing the eNISTmAb in which the GTG codon was replaced by GTT resulted in substantial reduction in the truncated heavy chain (Figure 4, compare lane 2 to lane 1).

To test the purity of the eNISTmAb and to evaluate if the antibody produced was intact and properly folded, a gel-filtration analysis was used. The protein purified on Protein-A column was analyzed by a Superdex-200 gel filtration column (see Materials and Methods for details). As shown in Figure 5A, most of the eNISTmAb eluted as a single peak with only a small "shoulder" and a few peaks of smaller molecular mass, suggesting that only a small fraction of the eNISTmAb was not fully assembled. However, when the peak fraction was analyzed by non-reducing SDS-PAGE, several bands could also be observed. Some of these additional bands are likely due to alternative or incomplete disulfide bond formation, as was shown for the mammalian-expressed NISTmAb.[26]

Production and purification of the labeled eNISTmAb

M9 minimal media[27] was used as the basis for labeling the eNISTmAb. For ^{15}N labeling, unlabeled ammonium chloride was replaced with ^{15}N ammonium chloride. For ^{13}C labeling, unlabeled glucose was replaced with ^{13}C labeled glucose. Deuterium (^{2}H) labeled mAb was produced by growing cells in deuterated water ($^{2}H_2O$). eNISTmAb labeled with ^{15}N, ^{13}C, and ^{2}H was produced by growing the cells in M9 media made in $^{2}H_2O$ and supplemented with ^{15}N ammonium chloride and ^{13}C-labeled glucose. Labeled proteins were purified on CaptureSelect

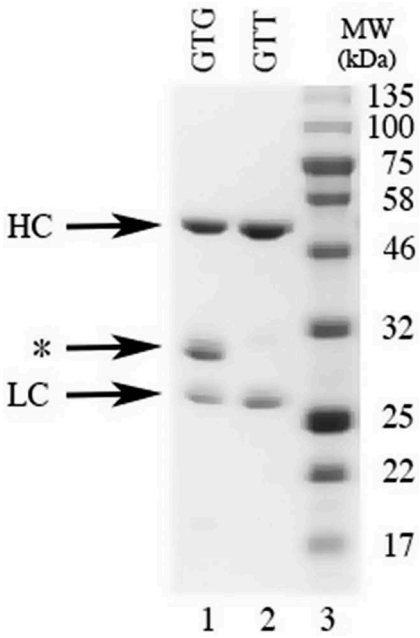

Figure 4. The effect of the GTG to GTT substitution at the rare initiation site on the expression of the eNISTmAb.

SDS-PAGE analysis of the eNISTmAb after purification on Protein-A. Lane 1 is the purified protein after expression from the clone in which GTG encodes for V_{214}. Lane 2 is the purified protein after expression from the clone in which GTT encodes for V_{214}. Five micrograms of each protein were separated on a 12% SDS-PAGE followed by staining with Coomassie Brilliant Blue R-250. Lane 3, molecular weight marker (kDa); HC, heavy chain; LC, light chain, *, truncated heavy chain.

CH1 resin (see Materials and Methods for details). Regardless of the labeling scheme, the yields were about 1 mg/L of purified eNISTmAb, with the only observed contaminant being the truncated product described above (Fig. S4).

Mass analysis of unlabeled and labeled eNISTmAbs

Matrix Assisted Laser Desorption/Ionization (MALDI) mass spectrometry analysis was used to determine the extent of stable isotope incorporation. Since mAbs produced in *E. coli* are not glycosylated, the only difference in mass between the labeled and unlabeled proteins was expected to be due to the incorporation of ^{15}N, ^{13}C, and nonexchangeable ^{2}H. As the proteins were purified in buffer containing hydrogenated water, only the nonexchangeable hydrogens retain deuterium. The percent incorporation of the individually labeled ^{13}C, ^{15}N and ^{2}H were 95%, 96% and 82%, respectively (Fig. S5) similar to those with other proteins expressed in *E. coli* under similar conditions (for example, see Ref. [28]).

Higher order structural assessment of the labeled eNISTmAb by 2D-NMR

The higher order structure (HOS) of proteins, including biologics, can be evaluated at the atomic level by high-resolution, two-dimensional (2D) $^{1}H,^{13}C$ and $^{1}H,^{15}N$ heteronuclear NMR spectra.[21,29–36] The appropriate 2D-NMR method was applied to each eNISTmAb sample, *e.g.*, $^{1}H,^{13}C$ constant time (CT) heteronuclear single quantum coherence spectroscopy (HSQC) for the U-^{13}C sample; $^{1}H,^{15}N$ gradient-selected (g)HSQC for the U-^{15}N sample, and both methods for the triply-labeled $^{2}H,^{13}C,^{15}N$ sample (Figure 6, Fig. S6). In all cases, the 2D spectral maps show that all eNISTmAb isotope-enriched samples were properly folded in one predominant conformation or averaged conformational ensemble. Overlaying the 2D $^{1}H,^{13}C$ CT-HSQC spectra of the triply-labeled $^{2}H,^{13}C,^{15}N$ eNISTmAb with the unlabeled NISTmAb afforded many spectral similarities, yet significant spectral differences likely arose from the lack of glycosylation on the eNISTmAb and the Met residue at the N-termini of the light and heavy chains (Fig. S6 Panel A).

To pinpoint the observed spectral differences to the Fc domain, 2D $^{1}H,^{13}C$ gHSQC spectra were recorded for both the NIST-Fab and NIST-Fc derived from papain cleavage of the NISTmAb (Fig. S6, Panels B and C). An overlay of the isolated NIST-Fab domain with the intact eNISTmAb reveals that most NIST-Fab signals show a high degree of overlap with the signals of the eNISTmAb, suggesting high structural similarity between the two Fab domains (Fig. S6, Panel B). Conversely, the overlay of the isolated NIST-Fc spectrum with the intact eNISTmAb shows many peaks significantly shifted, localizing the majority of spectral differences to the Fc domain (Fig. S6, Panel C). Moreover, the eNISTmAb does not have any cross peaks arising from methyls of the N-acetylglucosamine (GlcNAc) as would be expected for an aglycosolyated mAb. In total, the observed spectral shifts in the $^{1}H,^{13}C$ eNISTmAb spectra can be tentatively assigned to the lack of glycosylation of the eNISTmAb and the resulting effects on Fc structure from the lack of glycosylation.[21]

Discussion

Stable isotope labeling of proteins using *E. coli* expression platforms has several advantages when compared to other expression systems. One significant benefit is substantial reduction in media costs. While it is possible to label proteins with ^{13}C and ^{15}N in mammalian cells, substitution of labeled amino acids in complex cell culture media is required, since viable growth of mammalian cells in minimal media is currently not possible. In addition, fractional, "random" incorporation of ^{13}C into protein (less than 100%) is advantageous for some NMR applications.[37] In the case of mammalian expression systems, commercially available amino acids are uniformly ^{13}C-labeled, and fractional ^{13}C-labeling would only be possible with specialty synthesis of fractionally labeled amino acids. The other major advantage of expression in *E. coli* is the ability to achieve high levels of deuteration of protein. While *E. coli* can be grown in media containing 100% $^{2}H_2O$ and deuterated carbon sources to achieve perdeuration levels of up to ~ 98%, in our experience mammalian cells are not viable in media containing more than 35% $^{2}H_2O$ (data not shown). Deuteration of proteins enables the application of many sophisticated NMR methods for spectral assignment and structure/dynamic analysis to mAbs by eliminating efficient NMR relaxation pathways involving ^{1}H atoms, and thus reducing NMR line widths and increasing spectral intensities for these high molecular weight proteins.[38] Deuteration also enables application of contrast matching approaches to facilitate studies of multicomponent and complex protein assemblies using neutron scattering (for example, see Ref.[39]).

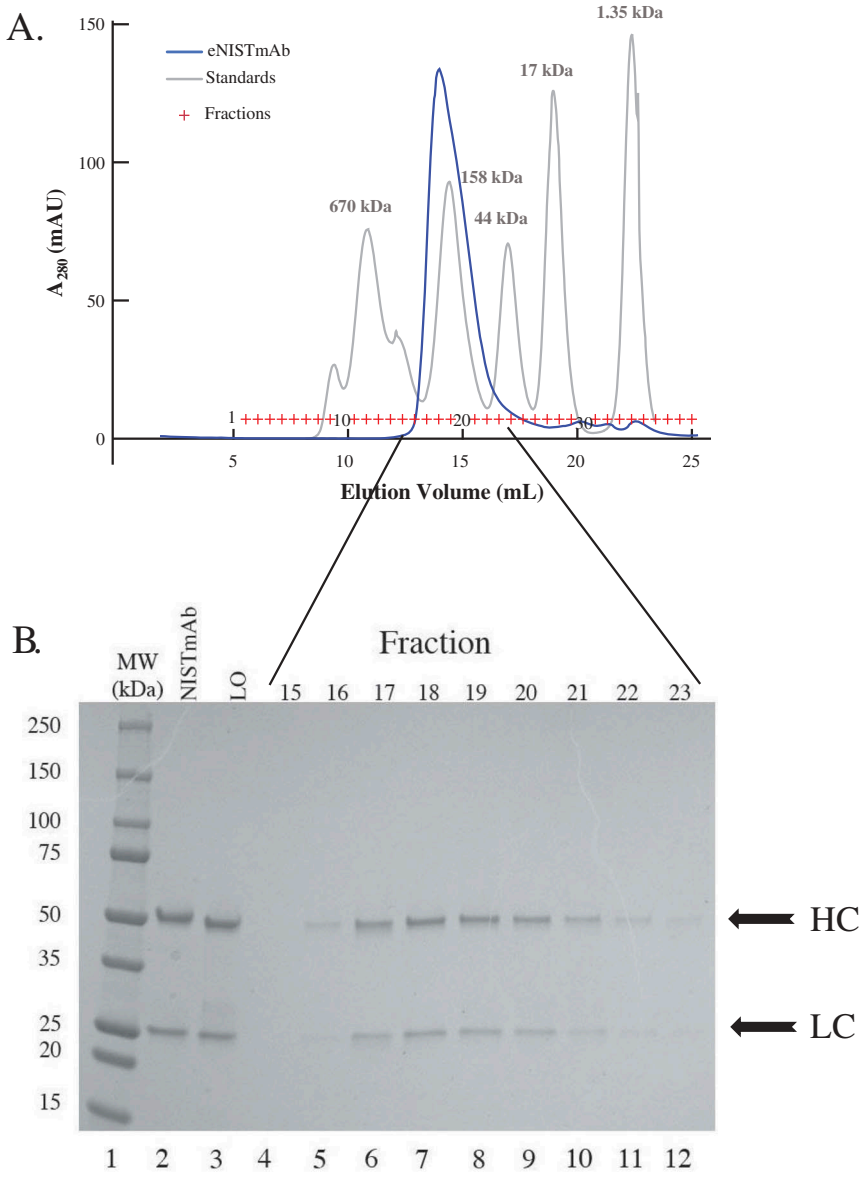

Figure 5. The eNISTmAb forms a tetrameric complex.

A) The eNISTmAb protein solution (300 µg) and molecular mass standards were subjected to Superdex-200 gel filtration analysis. The protein concentration in each eluted fraction was measured by ultraviolet absorption at 280nm. Blue, eNISTmAb; green, molecular mass standards. B) Proteins in aliquots (20 µL) from each indicated fraction were separated by electrophoresis through 4% – 20% SDS-PAGE and stained with Coomassie Brilliant Blue R-250. Lane1, molecular mass standards (kDa); lane 2, NISTmAb; lane 3, load on sample of eNISTmAb; lanes 4–12, column fractions. HC, heavy chain; LC, light chain.

The *E. coli*-expressed full-length mAbs are aglycosylated and therefore cannot function in all respects, such as FcγR receptor binding, as would be expected from the same mAb expressed in mammalian cells with glycosylation. However, one can bypass some of the requirements for glycosylation by genetically engineering two previously isolated point mutations (E382V/M428I)[40] in the conserved Fc region of IgG. The resulting variant aglycsoylated IgG expressed in SHuffle can indeed bind efficiently to its cognate FcγR receptor protein.[14] Intriguingly, it has been shown that the glycosylation machinery can be transferred to *E. coli*, resulting in *E. coli* cells capable of N-glycosylation of proteins.[41–43] Introduction of this machinery into *E. coli* SHuffle cells may enable the production of N-glycosylated antibodies. Such an improvement would afford a mAb more similar to its mammalian-expressed therapeutic counterpart. However, since the Fab is not glycosylated for many therapeutic mAbs, the isotopically-labeled Fab expressed from the current *E. coli* SHuffle cell platform described in this report is more representative of therapeutic Fabs produced from mammalian cells. Since the Fab is shorter than the full-length antibody, it can be expressed and purified with good yield.[44] The marketed products ranibizumab (Lucentis®)[45] and certolizumab pegol (Cimzia®)[46] are Fabs made using *E. coli*.

An *E. coli* expression platform for the robust production of isotopically-labeled mAbs is especially beneficial in expanding

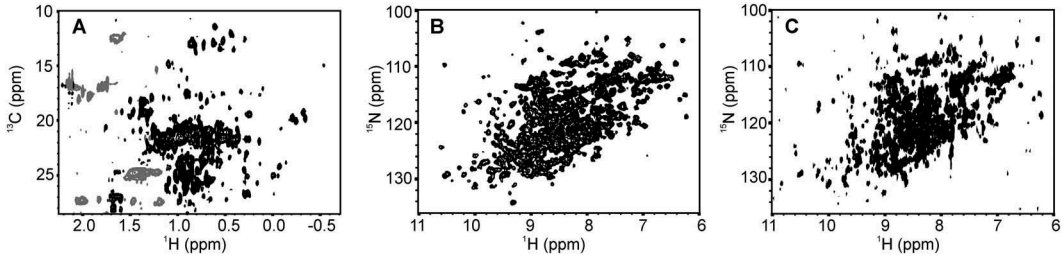

Figure 6. 2D-NMR spectral maps of various isotopically enriched eNISTmAbs.
A) ^{1}H,^{13}C CT-HSQC of the 25 µM uniformly ^{13}C-enriched sample; B) ^{1}H,^{15}N SOFAST-HMQC of the 25 µM uniformly enriched ^{15}N sample; C) ^{1}H,^{15}N gHSQC of the 10.6 µM triply enriched ^{2}H, ^{13}C, ^{15}N sample. Protein samples were constituted in 25 mM bis tris-*d19*, pH 6.0, and spectra were recorded at 50°C. Positive contours are in black and negative contours in gray.

the application of NMR and SANS in biopharmaceutical development and manufacture. NMR is increasingly used during biopharmaceutical development, including discovery, drug design and optimization, formulation development, aggregation and impurity analysis, and has been thoroughly reviewed.[36,47–49] More recently, the 2D-NMR method is becoming more established as a tool for assessing mAb HOS.[33,35,50,51] However, in the absence of resonance assignments 2D-NMR spectra can only be used as a composite high resolution structural fingerprint. The *E. coli* expression described herein provides an assessable platform to label a mAb with stable isotopes. This technological development will allow the implementation of NMR methods to assign ^{1}H,^{15}N and,^{1}H,^{13}C resonances, which allows 2D-NMR cross peak patterns to be correlated and interpreted in terms of specific amino acids within the mAb primary sequence. Such analysis will provide the ability to assess the structural impact of a range of parameters, including post-translational modifications such as methionine oxidation.[52] In the case study of the small protein therapeutic filgrastim, resonance assignments allowed a detailed mapping of the structural effects for different formulation conditions.[53] For mAb therapeutics, the isolated Fab and Fc are known to retain a similar HOS to that observed for these fragments in the intact NISTmAb.[30] Once resonance assignments are made for Fabs, which can be generated at higher yield than the intact mAb using the *E. coli* platform, they can be directly transferred to the Fab domain of the intact molecule. Once this is accomplished, any observed chemical shift perturbations can be traced to specific amino acids, thus potentially enabling a more precise determination of the source of the HOS deviation.

One of the key advantages of neutron scattering over X-ray and other structural methods is the technique of contrast variation, which provides the ability to resolve the structural properties of individual components of a complex system. The inherent differences in scatter length densities vary between different classes of biomolecules including protein, nucleic acids and lipids. These allow structural studies of complex systems of combinations of proteins, lipids and nucleic acids by varying the H_2O:$^{2}H_2O$ ratio in the solvent. However, to distinguish between components of a system in which the scattering length densities are all similar (*i.e.*, protein-protein complexes), deuterium labeling of the material is required. Therefore, the studies of structure and dynamics of mAb using SANS are substantially enhanced by deuteration of the material.

Stable isotope labeled internal standards for mass spectrometry-based approaches also show significant promise for improving quantitative structural readouts. While label-free methods for MS-based quantitation are becoming increasingly successful, the use of stable isotope labeled internal standards have historically provided higher accuracy and precision and are required for absolute quantitative methods for pharmacokinetic studies.[54,55] For example, isotopic labels were introduced into one mAb by adding ^{13}C6-lysine and ^{13}C6-arginine to the cell-culture medium.[56] In this report, the use of the labeled mAb as an internal reference standard in mass spectrometry-based peptide mapping showed reproducible quantification and the ability to quantitatively identify differences in post-translational modifications (PTMs).[56] Since physicochemical properties of labeled and natural peptides, including MS signal response, are largely the same, quantitation via relative MS signal intensities of labeled and unlabeled peptides therefore allows more consistent relative and/or absolute quantitation.

Here we describe, for the first time, the expression and purification of stable isotopically labeled mAb in an engineered *E. coli*. The use of a single column affinity purification followed by size exclusion chromatography (SEC) resulted in pure, well-folded mAb. Although the *E. coli*-expressed mAbs are not glycosylated, they share many of the structural features of their mammalian counterparts. Therefore, they provide a useful research tool for investigating mAb structure and dynamics.

Materials and Methods

Gene synthesis and plasmid construction

The genes encoding for the heavy and light chains of the eNISTmAb were synthesized at GeneArt Gene Synthesis and obtained as a gene cloned into the Bgl II and Bpu1102 I/Blp I restriction endonuclease sites of pET-21a vector (Merck Millipore, 69740-3) (Fig. S7). The construct contained the DNA sequence encoding the heavy and light chains of the eNISTmAb, each with a promoter (cyan in Fig. S7), its own regulatory sequences and transcription termination signal (gray in Fig. S7). The plasmid was transformed into *E. coli* SHuffle T7 express cells (New England Biolabs, C3029J) and

selected on Luria-Bertani (LB) agar media containing 100 μg/mL ampicillin (Sigma-Aldrich, A9518). Incubation of cells post transformation and subsequent growth was at 30°C as specified by the supplier.

eNISTmAb production in LB media

A single colony was grown overnight at 30°C in 5 mL of LB media supplemented with 100 μg/mL ampicillin. Five hundred mL of LB/amp were inoculated with the overnight culture and grown at 30°C until OD_{600} of about 0.7. At this stage of growth, isopropyl-β-D-thiogalactopyranoside (IPTG) (Sigma-Aldrich, I6758) was added to a final concentration of 1 mM, and mAb production was induced overnight at 30°C. Cells were harvested at 10,000 x g for 20 min and washed with phosphate buffered saline (PBS) (pH 7.4, 137 mM NaCl, 2.68 mM KCl, 10.14 mM Na_2PO_4, 1.76 mM KH_2PO_4). Cell pellet was immediately used for mAb purification, or the cells were kept at −70°C until used.

eNISTmAb production in minimal media

Minimal media was prepared as described by Davis et al.[27] The composition of the media was: 6 g Na_2HPO_4, 3 g KH_2PO_4, 0.5 g NaCl, 1 g NH_4Cl, 246 mg $MgSO_4•7H_2O$ and 5 g glucose per L. Ampicillin was added to a final concentration of 50 μg/mL. *E. coli* SHuffle cells harboring pET-21a/eNISTmAb recombinant plasmid were grown at 30°C for 24 h on minimal media agar plate containing 50 μg/mL ampicillin. A colony was transferred to 10 mL minimal media containing 50 μg/mL ampicillin, and the cells were grown overnight at 30°C with shaking at 250 RPM. This inoculum was transferred to 100 mL minimal media containing ampicillin as described above. This culture was grown again overnight at 30°C. Next, this seed culture was transferred to 900 mL of minimal media containing ampicillin in a 2 L flask. This culture was grown at 30°C for about 7 h until OD_{600} of about 0.7. eNISTmAb production was induced with 1 mM IPTG at 30°C for about 15 h. Cells were harvested at 10,000 x g for 20 min and washed with PBS. The wet weight of cells obtained in this procedure was about 2 g/L culture, and a total of two liters of culture were produced.

Production of ^{15}N or ^{13}C uniformly labeled eNISTmAb

Growth of cells for the production of ^{15}N- or ^{13}C-labeled eNISTmAb was identical to that described for the unlabeled mAb in minimal media except that ^{15}N-NH_4Cl (Cambridge Isotope Laboratories, NLM 467) replaced NH_4Cl, and ^{13}C-glucose (Cambridge Isotope Laboratories, CLM 1396) replaced glucose. The wet weight of cells in each case was about 2 g/L culture.

Production of deuterium (^2H)-labeled and ^{15}N, ^{13}C, ^2H (triply)-labeled eNISTmAb

Growth of *E. coli* cells in minimal media with 100% deuterium (deuterium oxide, ^2H_2O) (Sigma-Aldrich, 756,822) is impeded if that amount of deuterium is present at the start of incubation.[28] Hence, the cells must be acclimated slowly to the increasing concentration of deuterium to enable final growth of cells in 100% ^2H_2O. Acclimatization of cell growth in ^2H_2O was achieved as follows. Minimal media was prepared in 25%, 50%, 75%, and 100% ^2H_2O, each containing 50 μg/mL ampicillin. Loops full of cells grown in 100% H_2O minimal media were used as inoculum; the cells in 5 mL of minimal media in 25% ^2H_2O were then grown at 30°C for 24 h. Next, 5 mL of minimal media in 50% ^2H_2O was inoculated with 0.1 mL of cells grown in 25% ^2H_2O. Cells were grown at 30°C for 24 h. Next, 5 mL of minimal media in 75% ^2H_2O was inoculated with 0.1 mL of cells grown in 50% ^2H_2O. Cells were grown at 30°C for 16 h. A final round of growth in minimal media in 100% ^2H_2O was achieved by inoculating 0.1 mL of cells grown in 75% ^2H_2O into 5 mL of minimal media in 100% ^2H_2O. Cells had to be grown for about 50 h at 30°C to reach OD_{600} of about 1.0. These cells were stored in 20% glycerol at −70°C for further use as fully acclimatized cells.

Production of ^{15}N, ^{13}C, ^2H (triply)-labeled eNISTmAb was achieved by growing cells in minimal media prepared in ^2H_2O containing ^{15}N-NH_4Cl and ^{13}C-glucose and 50 μg/mL ampicillin. A loop full of glycerol stock of ^2H_2O-acclimatized cells were grown in 10 mL of this media at 30°C. After about 50 h growth, the 10 mL culture was transferred to 200 mL of triply labeled minimal media. Growth continued at 30°C for about 30 h. Two 1 L triply labeled minimal media were each inoculated with 100 mL of fresh culture and grown at 30°C for 20 h. At this time, when OD_{600} was about 0.7, IPTG was added to a final concentration of 1 mM and induced at 30°C for about 16 h. Cells were harvested and washed with PBS. The wet weight of triply labeled cells was about 2 g/L culture.

Purification of unlabeled and labeled eNISTmAb

The procedure described below for the purification of mAb from all five types of cells, (unlabeled, ^{15}N labeled, ^{13}C labeled, ^2H, labeled, and ^{15}N, ^{13}C, ^2H triply labeled), is identical. Four grams wet weight of cells, from 2 L cell culture, were suspended in 20 mL of PBS supplemented with 5 mM EDTA and a tablet of protease inhibitor cocktail (Sigma-Aldrich, S8830). Cell suspension was passed through a French Press at 10,000 PSI. Cell-free extract was centrifuged at 30,000 x g for 30 min. Protein-A resin (0.5 mL, MabSelect SuRe, GE Healthcare Life Sciences, 17-5280-01) was equilibrated with PBS in a 25 mL polypropylene column, and the supernatant was added to the resin. The column was plugged at both ends and kept on a rocker with end-to-end rotation for 2 h at 4°C to capture the mAb through the Fc region. The column was briefly centrifuged at 200 x g to pull-down the resin, and the supernatant was let through. Resin was washed three times with 10 mL PBS each time. The mAb was eluted successively with four 1 mL aliquots of 0.3 M sodium citrate, pH 3.0. The effluent was collected into tubes containing 0.2 mL of 1 M Tris-HCl, pH 9.0 to neutralize the acid condition of the elution buffer. Purified fractions were analyzed by SDS-PAGE and visualized by staining with Coomassie Brilliant Blue R-250 (Sigma-Aldrich, B7920). The mAb was also purified by binding to CaptureSelect IgG-CH1 affinity matrix (Thermo Fisher

Scientific, 194320005) resin under identical conditions as described above.

eNISTmAb purification on size-exclusion chromatography

In addition to the expected full-length heavy chain, a truncated product of the heavy chain of about 27 kDa was observed on SDS-PAGE (Figure 1, lanes 1 and 2) following purification of mAb on MabSelect SuRe (Protein-A) resin (Figure 1, lane 1) or CaptureSelect CH1 resin (Figure 1, lane 2). In order to obtain pure mAb, the effluent from MabSelec SuRe resin was further purified by SEC on an HPLC Biosep 3000 column (60 x 20 mm) from Phenomenex. The column was equilibrated and eluted with PBS at 1.5 mL/min at 22°C. Three mL fractions were collected and analyzed on SDS-PAGE (Figure 1, lane 3). The first three fractions, which appeared to be pure, were pooled.

eNISTmAb analysis using analytical size-exclusion chromatography

Three hundred micrograms of eNISTmAb and Gel Filtration standards (Bio-Rad, 151–1901) were dissolved in 400 µL of PBS and loaded onto a Superdex-200 column (HR10/30; GE Healthcare) pre-equilibrated in the same buffer. Fractions (500 µL) were collected from the column at a flow rate of 0.5 mL/min. The proteins present in aliquots (20 µL) of each fraction were separated by electrophoresis through a 4% – 20% polyacrylamide–SDS gel (Bio-Rad, 4561096) and stained with Coomassie Brilliant Blue (R250).

Sample preparation for NMR spectroscopy

The NISTmAb was used as the NMR spectral benchmark for the eNISTmAb. All NIST-Fabs and NIST-Fcs were prepared by papain digestion according to a previous report.[30] All NISTmAb, NISTmAb fragments, and eNISTmAb samples were buffer exchanged four times into 25 mM bis-tris-*d19* pH 6.0 using a 30 kDa Amicon centrifugal filter (EMD Millipore, UFC800324). The final protein concentration was 300 µM for NISTmAb and 25 µM for eNISTmAb (10.6 µM for the triply labeled sample), all with a final volume of 300 µL.

2D-NMR spectroscopy

All spectra were measured on a 900 MHz NMR spectrometer (Bruker BioSpin) equipped with a triple resonance cryogenically-cooled TCI probe with a z-axis gradient system. 2D $^{1}H,^{15}N$ gHSQC were collected at 50°C on the triply labeled eNISTmAb sample. The spectrum was acquired with 50% non-uniform sampling (NUS) with the NUS schedule determined by the Poisson Gap algorithm.[57] The spectral width was 38 ppm by 18 ppm, corresponding to acquisition times of 18.4 ms (128 total reconstructed points) and 100 ms (3,244 total points), in the ^{15}N and ^{1}H dimension respectively. The ^{15}N and ^{1}H transmitters were placed at 117 ppm and on water, respectively. The inter-scan delay was 1.5 s, and 512 scans per transient were collected.

For the U-^{15}N labeled sample, the $^{1}H,^{15}N$ spectral map was acquired with the Selective Optimized Flip Angle Short Transient (SOFAST)-Heteronuclear Multiple Quantum Coherence spectroscopy (HMQC) pulse sequence us 50% NUS. A Pc90 excitation pulse and a Reburp refocusing pulse were applied at 8.25 ppm with a bandwidth of 5000 Hz. The recycling delay was 0.4 s, 512 scans per transient were collected, and the ^{1}H acquisition time was set to 50 ms. All other experimental parameters were the same as the $^{1}H,^{15}N$ gHSQC.

For the U-^{13}C eNISTmAb sample, a $^{1}H,^{13}C$ CT-HSQC was recorded at 50°C with 50% NUS and a spectral width was 30 ppm by 14 ppm, corresponding to 128 total reconstructed points by 2,522 total points in the ^{13}C and ^{1}H dimensions, respectively. The ^{13}C and ^{1}H transmitters were placed at 20 ppm and on water, respectively. The constant time period was 13.3 ms; too much signal was lost due to T2 relaxation if the CT period was set to the full 26.6 ms (data not shown). The inter-scan delay was 1.5 s, and 128 scans per transient were collected.

For the $^{1}H,^{13}C$ gHSQC on the intact NISTmAb, NIST-Fab, and NIST-Fc, the spectra were acquired with uniform sampling and a spectral width was 30 ppm by 14 ppm, corresponding to acquisition times of 9.4 ms (128 total points) and 100 ms (2,522 total points), in the ^{13}C and ^{1}H dimension, respectively. The ^{13}C and ^{1}H transmitters were respectively placed at 20 ppm and on water. The inter-scan delay was 1.5 s, and 256 scans per transient were collected.

The spectra were apodized with a shifted sine-square bell function, zero-filled and reconstructed using the iterative soft thresholding algorithm within nmrPipe V8.9.[58] All uniformly sampled spectra were linear predicted in the ^{13}C dimension to double the number of points before Fourier Transform. The resulting spectra were visualized using NMRFAM-SPARKY V1.4.[59]

Liquid chromatography-mass spectrometry analysis (LC-MS)

To separate the polypeptide chains, 1.5 µg of protein was reduced by incubating in 10 mM DTT for 30 minutes at room temperature. The reduced sample was diluted to 75 ng/µL in 0.1% formic acid/water, then analyzed by reverse phase liquid chromatography (LC) and electrospray ionization time-of-flight mass spectrometry (ESI-TOF MS). Four µL (300 ng) of sample were injected into an HPLC-Chip Cube (Agilent Technologies) via an Agilent 1200 series nano LC and separated with a custom reverse phase HPLC-chip containing an integrated trapping column (40 nL capacity), separation column and nano-ESI emitter (75 µm x 150 mm, both packed with PLRP-S, 5 µm particles, 1000 Å pore size).[50] The trapping column was loaded at 4 µL/min and the separation column developed at a flow rate of 600 nL/min. The column was equilibrated for two minutes in 95% mobile phase A, 5% mobile phase B (A: 0.1% formic acid in water; B: 0.1% formic acid in acetonitrile). The protein was then eluted over 15 minutes with a linear gradient from 5% to 95% B and analyzed on an Agilent 6210 ESI-TOF mass spectrometer. The protein was found to elute approximately 10 minutes after injection. The mass spectra were acquired from 100 m/z to 3200 m/z, one cycle/sec and 10,000 transients per scan using an ionization

energy of 1900 V, fragmentor of 215 V and drying gas of 325°C at 5.0 L/min. The acquired spectra were extracted and the protein deconvoluted with Agilent MassHunter Qualitative Analysis Software (with Bioconfirm) B 2.0.2 software using a mass range of 10 kDa to 70 kDa.

Liquid chromatography-tandem mass spectrometry analysis (LC-MS/MS)

The suspected truncated heavy chain fragment was excised from a Coomassie-stained SDS-PAGE for in-gel protein digestion and mass spectrometry analysis. The gel band was sliced into 1 mm^3 pieces, destained, reduced, and alkylated with iodoacetamide. The band was then digested with Trypsin-ultra, Mass Spectrometry Grade (New England Biolabs, P8101) at a concentration of 2 ng/μL per band for one hour at 50°C. Extracted peptides were acidified to 0.5% trifluoroacetic acid (TFA) for mass spectrometry analysis.

One-tenth of the extracted peptides (5 μL) was loaded via Proxeon Easy-nLC II (Thermo Fisher) onto a 20 cm x 100 μm ID reverse phase C18 analytical column (New Objective Picofrit), self-packed with 3 μm Aqua C18 (Phenomenex). Peptides were eluted at a flow rate of 300 nL/min over a 45-minute 5% to 35% B gradient (mobile phase A: 0.1% formic acid/water, mobile phase B: 0.1% formic acid/acetonitrile), followed by a 5 min gradient to 70% B, then isocratic for 5 min at 70% B. Peptides were analyzed on an LTQ Orbitrap XL with electron transfer dissociation (ETD) mass spectrometer (Thermo Fisher) using both collision-induced dissociation (CID) with a normalized collision energy of 35.0 and ETD fragmentation. Full scan spectra were collected from 400 m/z to 1600 m/z with a resolution of 30,000. Data-dependent settings included dynamic exclusion set at 30 sec, rejection of +1 charge states, and the top 3 peaks were analyzed by MS/MS.

The resultant MS/MS spectra were analyzed using PEAKS 7.5 software (Bioinformatics Solutions, Inc., Waterloo, Ontario). The data were searched against a custom *E. coli* database appended with eNISTmAb sequences, allowing for carbamidomethylation (CAM)-modification of cysteines (fixed modification), oxidation of methionines (variable modification), and two missed cleavages. The precursor mass tolerance was set to 20 ppm, and the fragment mass tolerance was set to 0.6 Da. The data were filtered to a 1% false discovery rate and at least one unique peptide per protein.

N-terminal sequencing of the truncated form of the heavy chain

The truncated heavy chain band was transferred to poly-vinyl-i-dene difluoride membrane and was sent for N-terminal Edman degradation to Alphalyse Inc. (Palo Alto, CA).

Mass spectrometry analysis of labeled eNISTmAb

A Bruker Microflex LRF MALDI in linear positive mode was used for all measurements. Calibration was done using Bruker Protein Calibration Standards II (Bruker, 8207234) and phosphorylase B (Sigma-Aldrich, P6635). Bruker standards were prepared as per the manufacturer's recommendation. Phosphorylase B was prepared as a 5 mg/mL stock in 0.1% TFA (Sigma-Aldrich, T3693). All calibrations and data collation were performed using 2,5-dihydroxyacetophenone (DHAP) matrix (Bruker, 8231829). The matrix was prepared by dissolving 7.5 mg of DHAP in 375 μL ethanol. Just prior to use, an aqueous solution of 18 mg/ml diammonium hydrogen citrate (DAC) was added to the ethanol DHAP solution at a ratio of 1:3. For each sample, 2 μL of protein (about 2 μg) was mixed with 2 μL of a 2% TFA solution. Then, 2 μL of the fresh DHAP/DAC matrix solution was added and gently mixed. Once the mixture began to turn opaque, 1 μL was spotted onto a ground steel target. The target was then dried under vacuum for two minutes. Data collection and calibration were performed in liner positive mode using an 800 ms pulsed ion extraction (PIE). Data were recorded as $(M + 2H)^{2+}$ values. The percent incorporation was calculated from the intact mass of the labeled proteins as previously described.[5]

Acknowledgments

The authors would like to thank John Marino and John Schiel for their comments on the manuscript, Thomas Cleveland IV for his help with the analytical gel-filtration and Luke Arbogast for the deglycosylated NISTmAb. Certain commercial equipment, instruments, or materials are identified to adequately specify the experimental procedure. Such identification does not imply recommendation or endorsement by the National Institute of Standards and Technology, nor does it imply that the materials or equipment identified are necessarily the best available for the purpose.

Disclosure of Potential Conflicts of Interest

No potential conflict of interest was reported by the authors.

Funding

This work was supported by the National Institute of Standards and Technology (NIST).

ORCID

Colleen McClung http://orcid.org/0000-0002-0070-6033
Mehmet Berkmen http://orcid.org/0000-0002-9579-9745

References

1. Reichert JM. Marketed therapeutic antibodies compendium. mAbs. 2012;4:413–415. doi:10.4161/mabs.19931.
2. Schiel JE, Davis DL, Borisov O, American Chemical Society. State-of-the-art and emerging technologies for therapeutic monoclonal antibody characterization. Washington (DC, Oxford): American Chemical Society, Oxford University Press; 2014.
3. Chadd HE, Chamow SM. Therapeutic antibody expression technology. Curr Opin Biotechnol. 2001;12:188–194.
4. Reddy PT, Jaruga P, Nelson BC, Lowenthal MS, Jemth AS, Loseva O, Coskun E, Helleday T, Dizdaroglu M. Production, purification, and characterization of ^{15}N-labeled dna repair proteins as internal standards for mass spectrometric measurements. Methods Enzymol. 2016;566:305–332. doi:10.1016/bs.mie.2015.06.044.
5. Hoopes JT, Elberson MA, Preston RJ, Reddy PT, Kelman Z. Protein labeling in *Escherichia coli* with ^{2}H, ^{13}C, and ^{15}N. Methods Enzymol. 2015;565:27–44. doi:10.1016/bs.mie.2015.08.023.

6. Le MT, Brown RE, Simon AE, Dayie TK. *In vivo*, large-scale preparation of uniformly ^{15}N- and site-specifically ^{13}C-labeled homogeneous, recombinant RNA for NMR studies. Methods Enzymol. 2015;565:495–535. doi:10.1016/bs.mie.2015.07.020.
7. Mazor Y, Van Blarcom T, Iverson BL, Georgiou G. E-clonal antibodies: selection of full-length IgG antibodies using bacterial periplasmic display. Nat Protoc. 2008;3:1766–1777. doi:10.1038/nprot.2008.176.
8. Mazor Y, Van Blarcom T, Mabry R, Iverson BL, Georgiou G. Isolation of engineered, full-length antibodies from libraries expressed in *Escherichia coli*. Nature Biotechnol. 2007;25:563–565. doi:10.1038/nbt1296.
9. Simmons LC, Reilly D, Klimowski L, Raju TS, Meng G, Sims P, Hong K, Shields RL, Damico LA, Rancatore P, et al. Expression of full-length immunoglobulins in *Escherichia coli*: rapid and efficient production of aglycosylated antibodies. J Immunol Methods. 2002;263:133–147.
10. Zhou Y, Liu P, Gan Y, Sandoval W, Katakam AK, Reichelt M, Rangell L, Reilly D. Enhancing full-length antibody production by signal peptide engineering. Microb Cell Fact. 2016;15:47. doi:10.1186/s12934-016-0445-3.
11. Chan CE, Lim AP, Chan AH, MacAry PA, Hanson BJ. Optimized expression of full-length IgG1 antibody in a common *E. coli* strain. PLoS One. 2010;5:e10261. doi:10.1371/journal.pone.0010261.
12. Makino T, Skretas G, Kang TH, Georgiou G. Comprehensive engineering of *Escherichia coli* for enhanced expression of IgG antibodies. Metab Eng. 2011;13:241–251. doi:10.1016/j.ymben.2010.11.002.
13. Rouet R, Lowe D, Dudgeon K, Roome B, Schofield P, Langley D, Andrews J, Whitfeld P, Jermutus L, Christ D. Expression of high-affinity human antibody fragments in bacteria. Nat Protoc. 2012;7:364–373. doi:10.1038/nprot.2011.448.
14. Robinson MP, Ke N, Lobstein J, Peterson C, Szkodny A, Mansell TJ, Tuckey C, Riggs PD, Colussi PA, Noren CJ, et al. Efficient expression of full-length antibodies in the cytoplasm of engineered bacteria. Nat Commun. 2015;6:8072. doi:10.1038/ncomms9072.
15. Liu D, Cocco MJ, Rosenfied R, Lewis JK, Ren D, Li L, Remmele RL, Brems DN. Assignment of backbone ^{1}H, ^{13}C and ^{15}N resonances of human IgG1 Fc (51.4 kDa). Biomol NMR Assign. 2007;1:233–235. doi:10.1007/s12104-007-9065-5.
16. Lobstein J, Emrich CA, Jeans C, Faulkner M, Riggs P, Berkmen M. SHuffle, a novel *Escherichia coli* protein expression strain capable of correctly folding disulfide bonded proteins in its cytoplasm. Microb Cell Fact. 2012;11:56. doi:10.1186/1475-2859-11-56.
17. Ren G, Ke N, Berkmen M. Use of the SHuffle strains in production of proteins. Curr Protoc Protein Sci. 2016;85(5 26):1–5 1.
18. Schiel JE, Turner A. The NISTmAb reference material 8671 lifecycle management and quality plan. Anal Bioanal Chem. 2018;410:2067–2078. doi:10.1007/s00216-017-0844-2.
19. Schiel JE, Turner A, Mouchahoir T, Yandrofski K, Telikepalli S, King J, DeRose P, Ripple D, Phinney K. The NISTmAb reference material 8671 value assignment, homogeneity, and stability. Anal Bioanal Chem. 2018;410:2127–2139. doi:10.1007/s00216-017-0800-1.
20. Kadokura H, Katzen F, Beckwith J. Protein disulfide bond formation in prokaryotes. Annu Rev Biochem. 2003;72:111–135. doi:10.1146/annurev.biochem.72.121801.161459.
21. Arbogast LW, Delaglio F, Schiel JE, Marino JP. Multivariate analysis of two-dimensional ^{1}H, ^{13}C methyl NMR spectra of monoclonal antibody therapeutics to facilitate assessment of higher order structure. Anal Chem. 2017;89:11839–11845. doi:10.1021/acs.analchem.7b03571.
22. Reddy P, Peterkofsky A, McKenney K. Translational efficiency of the *Escherichia coli* adenylate cyclase gene: mutating the UUG initiation codon to GUG or AUG results in increased gene expression. Proc Natl Acad Sci U S A. 1985;82:5656–5660.
23. Romero A, Garcia P. Initiation of translation at AUC, AUA and AUU codons in Escherichia coli. FEMS Microbiol Lett. 1991;68:325–330.
24. O'Donnell SM, Janssen GR. The initiation codon affects ribosome binding and translational efficiency in *Escherichia coli* of cI mRNA with or without the 5′ untranslated leader. J Bacteriol. 2001;183:1277–1283. doi:10.1128/JB.183.4.1277-1283.2001.
25. Omotajo D, Tate T, Cho H, Choudhary M. Distribution and diversity of ribosome binding sites in prokaryotic genomes. BMC Genomics. 2015;16:604. doi:10.1186/s12864-015-1808-6.
26. Kashi L, Yandrofski K, Preston RJ, Arbogast LW, Giddens JP, Marino JP, Schiel JE, Kelman Z. Heterologous recombinant expression of non-originator NISTmAb. mAbs. 2018. in press. doi:10.1080/19420862.2018.1486355.
27. Davis RW, Botstein D, Roth JR, Cold Spring Harbor Laboratory. Advanced bacterial genetics. Cold Spring Harbor (N.Y.): Cold Spring Harbor Laboratory; 1980.
28. Duff AP, Wilde KL, Rekas A, Lake V, Holden PJ. Robust high-yield methodologies for ^{2}H and ^{2}H/^{15}N/^{13}C labeling of proteins for structural investigations using neutron scattering and NMR. Methods Enzymol. 2015;565:3–25. doi:10.1016/bs.mie.2015.06.014.
29. Arbogast LW, Brinson RG, Formolo T, Hoopes JT, Marino JP. 2D ^{1}H^{N,} ^{15}N correlated NMR methods at natural abundance for obtaining structural maps and statistical comparability of monoclonal antibodies. Pharm Res. 2016;33:462–475. doi:10.1007/s11095-015-1802-3.
30. Arbogast LW, Brinson RG, Marino JP. Mapping monoclonal antibody structure by 2D ^{13}C NMR at natural abundance. Anal Chem. 2015;87:3556–3561. doi:10.1021/ac504804m.
31. Brinson RG, Ghasriani H, Hodgson DJ, Adams KM, McEwen I, Freedberg DI, Chen K, Keire DA, Aubin Y, Marino JP. Application of 2D-NMR with room temperature NMR probes for the assessment of the higher order structure of filgrastim. J Pharm Biomed Anal. 2017;141:229–233. doi:10.1016/j.jpba.2017.03.063.
32. Aubin Y, Gingras G, Sauve S. Assessment of the three-dimensional structure of recombinant protein therapeutics by NMR fingerprinting: demonstration on recombinant human granulocyte macrophage-colony stimulation factor. Anal Chem. 2008;80:2623–2627. doi:10.1021/ac7026222.
33. Japelj B, Ilc G, Marusic J, Sencar J, Kuzman D, Plavec J. Biosimilar structural comparability assessment by NMR: from small proteins to monoclonal antibodies. Sci Rep. 2016;6:32201. doi:10.1038/srep32201.
34. Chen K, Park J, Li F, Patil SM, Keire DA. Chemometric methods to quantify 1D and 2D NMR spectral differences among similar protein therapeutics. AAPS PharmSciTech. 2018;19:1011–1019.
35. Ghasriani H, Hodgson DJ, Brinson RG, McEwen I, Buhse LF, Kozlowski S, Marino JP, Aubin Y, Keire DA. Precision and robustness of 2D-NMR for structure assessment of filgrastim biosimilars. Nature Biotechnol. 2016;34:139–141. doi:10.1038/nbt.3474.
36. Kiss R, Fizil A, Szantay C Jr. What NMR can do in the biopharmaceutical industry. J Pharm Biomed Anal. 2018;147:367–377. doi:10.1016/j.jpba.2017.07.004.
37. Wenrich BR, Sonstrom RE, Gupta RA, Rovnyak D. Enhanced biosynthetically directed fractional carbon-13 enrichment of proteins for backbone NMR assignments. Protein Expr Purif. 2015;115:1–10. doi:10.1016/j.pep.2015.08.005.
38. Pervushin K, Riek R, Wider G, Wuthrich K. Attenuated T2 relaxation by mutual cancellation of dipole-dipole coupling and chemical shift anisotropy indicates an avenue to NMR structures of very large biological macromolecules in solution. Proc Natl Acad Sci U S A. 1997;94:12366–12371.
39. Breyton C, Gabel F, Lethier M, Flayhan A, Durand G, Jault JM, Juillan-Binard C, Imbert L, Moulin M, Ravaud S, et al. Small angle neutron scattering for the study of solubilised membrane proteins. Eur Phys J E Soft Matter. 2013;36:71. doi:10.1140/epje/i2013-13071-6.
40. Jung ST, Reddy ST, Kang TH, Borrok MJ, Sandlie I, Tucker PW, Georgiou G. Aglycosylated IgG variants expressed in bacteria that selectively bind FcγRI potentiate tumor cell killing by monocyte-dendritic cells. Proc Natl Acad Sci U S A. 2010;107:604–609. doi:10.1073/pnas.0908590107.
41. Wacker M, Linton D, Hitchen PG, Nita-Lazar M, Haslam SM, North SJ, Panico M, Morris HR, Dell A, Wren BW, et al. N-linked

glycosylation in *Campylobacter jejuni* and its functional transfer into *E. coli*. Science. 2002;298:1790–1793. doi:10.1126/science.298.5599.1790.
42. Lizak C, Fan YY, Weber TC, Aebi M. N-linked glycosylation of antibody fragments in *Escherichia coli*. Bioconjug Chem. 2011;22:488–496. doi:10.1021/bc100511k.
43. Baker JL, Celik E, DeLisa MP. Expanding the glycoengineering toolbox: the rise of bacterial N-linked protein glycosylation. Trends Biotechnol. 2013;31:313–323. doi:10.1016/j.tibtech.2013.03.003.
44. Frenzel A, Hust M, Schirrmann T. Expression of recombinant antibodies. Front Immunol. 2013;4:217. doi:10.3389/fimmu.2013.00217.
45. Ferrara N, Damico L, Shams N, Lowman H, Kim R. Development of ranibizumab, an anti-vascular endothelial growth factor antigen binding fragment, as therapy for neovascular age-related macular degeneration. Retina. 2006;26:859–870. doi:10.1097/01.iae.0000242842.14624.e7.
46. Goel N, Stephens S. Certolizumab pegol. mAbs. 2010;2:137–147.
47. Wang G, Zhang ZT, Jiang B, Zhang X, Li C, Liu M. Recent advances in protein NMR spectroscopy and their implications in protein therapeutics research. Anal Bioanal Chem. 2014;406:2279–2288. doi:10.1007/s00216-013-7518-5.
48. Wishart DS. Characterization of biopharmaceuticals by NMR spectroscopy. Trends Analyt Chem. 2013;48:96–111. doi:10.1016/j.trac.2013.03.009.
49. Aubin Y, Freedberg DI, Keire DA. One- and two-dimensional NMR techniques for biopharmaceuticals. In: Houde DJ, Berkowitz SA, editors. Biophysical characterization of proteins in developing biopharmaceuticals. Boston (MA): Elsevier 2014. p. 341–382.
50. Amezcua CA, Szabo CM. Assessment of higher order structure comparability in therapeutic proteins using nuclear magnetic resonance spectroscopy. J Pharm Sci. 2013;102:1724–1733. doi:10.1002/jps.23531.
51. Arbogast LW, Brinson RG, Marino JP. Application of natural isotopic abundance ^{1}H-^{13}C- and ^{1}H-^{15}N-correlated two-dimensional NMR for evaluation of the structure of protein therapeutics. Methods Enzymol. 2016;566:3–34. doi:10.1016/bs.mie.2015.09.037.
52. Liu D, Ren D, Huang H, Dankberg J, Rosenfeld R, Cocco MJ, Li L, Brems DN, Remmele RL. Structure and stability changes of human IgG1 Fc as a consequence of methionine oxidation. Biochemistry. 2008;47:5088–5100. doi:10.1021/bi702238b.
53. Aubin Y, Hodgson DJ, Thach WB, Gingras G, Sauve S. Monitoring effects of excipients, formulation parameters and mutations on the high order structure of filgrastim by NMR. Pharm Res. 2015;32:3365–3375. doi:10.1007/s11095-015-1713-3.
54. Van Den Broek I, Niessen WM, Van Dongen WD. Bioanalytical LC-MS/MS of protein-based biopharmaceuticals. J Chromatogr B, Analyt Technol Biomed Life Sci. 2013;929:161–179. doi:10.1016/j.jchromb.2013.04.030.
55. Xu RN, Fan L, Rieser MJ, El-Shourbagy TA. Recent advances in high-throughput quantitative bioanalysis by LC-MS/MS. J Pharm Biomed Anal. 2007;44:342–355. doi:10.1016/j.jpba.2007.02.006.
56. Manuilov AV, Radziejewski CH, Lee DH. Comparability analysis of protein therapeutics by bottom-up LC-MS with stable isotope-tagged reference standards. mAbs. 2011;3:387–395.
57. Hyberts SG, Takeuchi K, Wagner G. Poisson-gap sampling and forward maximum entropy reconstruction for enhancing the resolution and sensitivity of protein NMR data. J Am Chem Soc. 2010;132:2145–2147. doi:10.1021/ja908004w.
58. Delaglio F, Grzesiek S, Vuister GW, Zhu G, Pfeifer J, Bax A. NMRPipe: a multidimensional spectral processing system based on UNIX pipes. J Biomol NMR. 1995;6:277–293.
59. Lee W, Tonelli M, Markley JL. NMRFAM-SPARKY: enhanced software for biomolecular NMR spectroscopy. Bioinformatics. 2015;31:1325–1327. doi:10.1093/bioinformatics/btu830.